Nanotechnology

Self-Assembly and Cross-Linking of Bionanoparticles at Liquid–Liquid Interfaces**

Justin T. Russell, Yao Lin, Alexander Böker, Long Su, Philippe Carl, Heiko Zettl, Jinbo He, Kevin Sill, Ravisubhash Tangirala, Todd Emrick, Kenneth Littrell, Pappannan Thiyagarajan, David Cookson, Andreas Fery, Qian Wang, and Thomas P. Russell**

The self-assembly of nanoscale materials to form hierarchically ordered structures promises new opportunities in optical, acoustic, electronic, as well as magnetic materials and devices.[1–4] Herein, we apply our recent findings on the self-assembly of nanoparticles at liquid interfaces,[5,6] based on Pickering emulsions,[7,8] to naturally occurring nanometer-scale structures. Bionanoparticles, such as viruses and other biological materials, are truly monodisperse in size and can be functionalized in a robust, well-defined manner.[9–12] These attributes afford a unique platform to investigate the mechanism and kinetics of self-assembly at the liquid–liquid interface quantitatively.

Numerous studies have focused on ordered 2D arrays of protein particles[13] by spreading and adsorbing proteins on surfaces[14,15] or at interfaces.[15–19] However, simple routes to direct and assemble bioparticles into 2D or 3D constructs with hierarchical ordering are still required. Herein, we use the interface between two immiscible liquids (that is, on the surface of droplets), which has been shown to be ideal for the assembly of colloidal and nanoscopic particles,[5–8,20–24] and chose the cowpea mosaic virus (CPMV) as a prototype. The CPMV is a non-enveloped plant virus that is approximately 30 nm in diameter and is isolated from infected black eye pea plants in yields of 1–2 g kg^{-1} of wet leaves.[25] The physical, biological, and genetic properties of the CPMV have been well characterized.[26–28] It consists of an icosahedral protein shell, or capsid, composed of 60 copies of the two different types of protein subunits.[29] CPMV particles are remarkably stable: they maintain their integrity for at least one hour at 50 °C (pH 7) and indefinitely at room temperature (pH 3.5–9). The CPMV was the first virus to be used in organic reactions and bioconjugation and has been studied extensively as a model system.[30–35] Multiple orthogonal reactive sites on the CPMV particles can be selectively functionalized under mild conditions, which is crucial for our self-assembly studies.

Wild-type CPMV (wt-CPMV) was labeled covalently with the fluorescent dye Oregon Green 488 or *N*,*N*,*N*′,*N*′-tetramethylrhodamine (Scheme 1), as described previously.[31] Perfluorodecalin droplets with diameters of 10–100 μm were obtained by dispersing perfluorodecalin in an aqueous buffer solution of fluorescently labeled CPMV particles. The CPMV particles segregated at the perfluorodecalin–water interface, thus stabilizing the dispersion of the oil droplets. Figure 1a shows a fluorescence confocal microscope image of perfluorodecalin droplets in a buffer solution containing 0.25 mg mL^{-1} of wt-CPMV. The particle assemblies of wt-CPMV at the droplet interface are clearly seen by the intense fluorescence at the droplet boundaries. The fluorescent background in the aqueous phase arises from excess virus particles in the buffer. The adsorption kinetics of the assembly process were monitored with a pendant-drop tensiometer. The particles assemble at the oil–water interface, thus leading to a reduction in the interfacial energy between the two phases and stabilization of the oil–water dispersion (Figure 1b). Tensiometric measurements under different bionanoparticle concentrations in the aqueous buffer phase suggest a characteristic timeframe for the assembly to reach monolayer adsorption.

Small-angle neutron scattering (SANS) was carried out using a stock solution of the CPMV (1.80 mg mL^{-1}) in a 100 mM potassium phosphate/D_2O buffer at pH 7.0. The SANS data from the dispersed CPMV bioparticles, the fitting

[*] L. Su, Professor Q. Wang
Department of Chemistry and Biochemistry
University of South Carolina
Columbia, SC 29208 (USA)
Fax: (+1) 803-777-9521
E-mail: wang@mail.chem.sc.edu

Y. Lin,[+] J. He, K. Sill, R. Tangirala, Professor T. Emrick, Professor T. P. Russell
Department of Polymer Science and Engineering
University of Massachusetts
Amherst, MA 01003 (USA)
Fax: (+1) 413-577-1510
E-mail: russell@mail.pse.umass.edu

J. T. Russell
Williston Northampton School
Easthampton, MA 01027 (USA)

Dr. A. Böker,[+] H. Zettl
Lehrstuhl für Physikalische Chemie II
Universität Bayreuth
95440 Bayreuth (Germany)

Dr. P. Carl, Dr. A. Fery
MPI für Kolloid und Grenzflächenforschung
Am Mühlenberg, 14424 Potsdam (Germany)

Dr. K. Littrell, Dr. P. Thiyagarajan
Argonne National Laboratory
IPNS-360, Argonne, IL 60439 (USA)

Dr. D. Cookson
Australian Synchrotron Research Program
Building 434
Argonne, IL 60439 (USA)

[+] equal contribution.

[**] This work was supported by the DOE (DE-FG-02-96ER45 and DE-FG02-04ER46126), the NSF for MRSEC at UMass Amherst (DMR 9400488), the Army Research Laboratory through the MURI program, the Max Planck Society, the DFG within the French–German Network on Complex Fluids, and the MAX KADE Foundation. This work benefited from Argonne's Advanced Photon Source (15-ID) and Intense Pulsed Neutron Source supported by the US Department of Energy, Basic Energy Sciences, Office of Science, under contract no. W-31-109-Eng-38. ChemMatCARS Sector 15 is principally supported by the National Science Foundation/Department of Energy under grant no. CHE0087817 and by the Illinois Board of Higher Education. Q.W. thanks the University of South Carolina and USC Nanocenter for financial support. A.F. and P.C. thank Helmuth Möhwald for stimulating discussions.

  DOI: 10.1002/ange.200462653

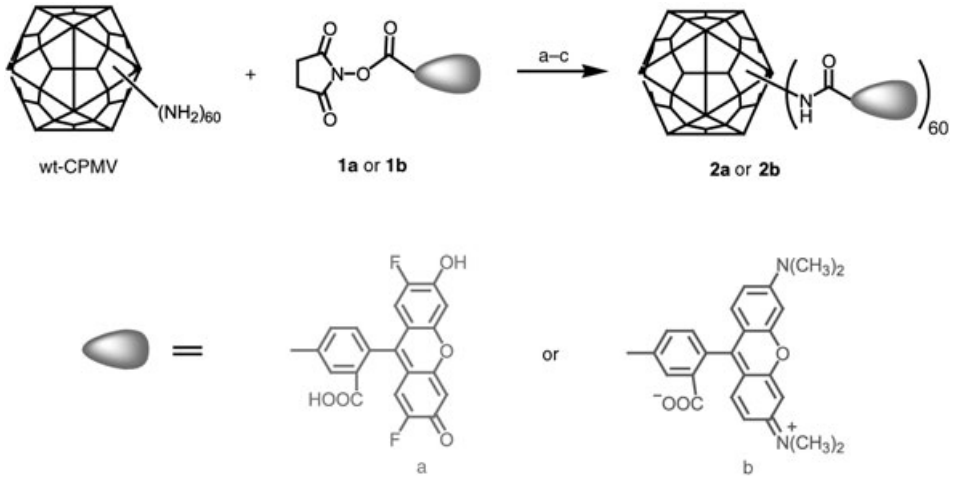

Scheme 1. Covalent labeling of wt-CPMV with fluorescent Oregon Green 488 or *N*,*N*,*N*′,*N*′-tetramethylrhodamine. a) 20% dimethyl sulfoxide (DMSO) in buffer, pH 7.0, 4 °C, 24 h; b) ultracentrifugation; c) dialysis.

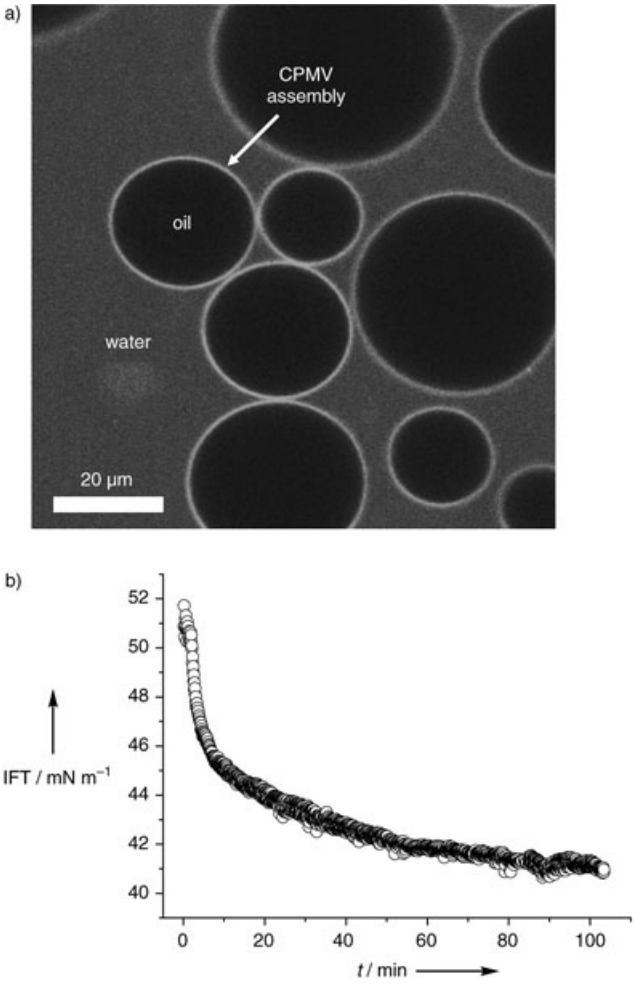

Figure 1. a) Confocal fluorescence microscope image of CPMV–particle assembly at perfluorodecalin droplets in water. b) Pendant-drop tensiometric data (interfacial tension (IFT) versus time) for the adsorption of CPMV particles from a buffered water phase (0.5 mg mL^{-1} CPMV in potassium phosphate buffer) to the perfluordecalin-drop interface.

with the spherical-shell form factor, and the resolution function for the small-angle neutron diffractometer (SAND) instrument are shown in Figure 2a. It is clear that the data are well described by a monodisperse system of spherical shells with an inner radius of 10.7 ± 0.1 nm and a wall thickness of 2.9 ± 0.1 nm; such a system is consistent with the structure of CPMV previously studied by Johnson and co-workers.[29]

The CPMV–particle assemblies were formed at interfaces by addition of perfluorodecalin (10 vol% in water) to the bioparticle in the buffer solutions (prepared by fivefold dilution of the stock solutions with the buffer) in a D_2O/H_2O mixture and shaken vigorously by hand to generate a microemulsion to contrast with the scattering from the perfluorodecalin. The composition of the D_2O/H_2O mixture was 0.313:0.687 (v/v (%)) and was chosen on the basis of the scattering length density of perfluorodecalin (4.18×10^{10} cm^{-2}), which was calculated by using the neutron scattering lengths of its atomic composition and a density of 1.908 g cm^{-3}.

The microemulsion samples were freshly prepared and kept at 6 °C for four hours for the interfacial assembly to attain equilibrium. The bionanoparticle-coated droplets were then accumulated and loaded into 2-mm sample cells. The SANS data were collected at 8 °C over 24 hours. The background-corrected SANS data for the CPMV–particle assemblies exhibit a power-law dependence of the form $I(q) \propto Q^{-2.5(\pm 0.3)}$, as shown by the solid line at low values of Q, where Q is related to the neutron wavelength λ and the scattering angle 2θ by the equation $Q = 4\pi \sin\theta/\lambda$ (Figure 2b). The average thickness t of the bionanoparticle assembly at the interfaces can be measured by using a modified Guinier approximation for sheetlike structures[36,37] [Eq. (1)].

$$I(Q) = Q^{-2} I_T \exp(-Q^2 R_t^2) \quad (1)$$

The thickness factor R_t can be determined from the slope of $\ln(Q^2 I(Q))$ versus Q^2 in an appropriate Q region where $Q_{max} R_t < 0.6$ and the thickness t can be derived from

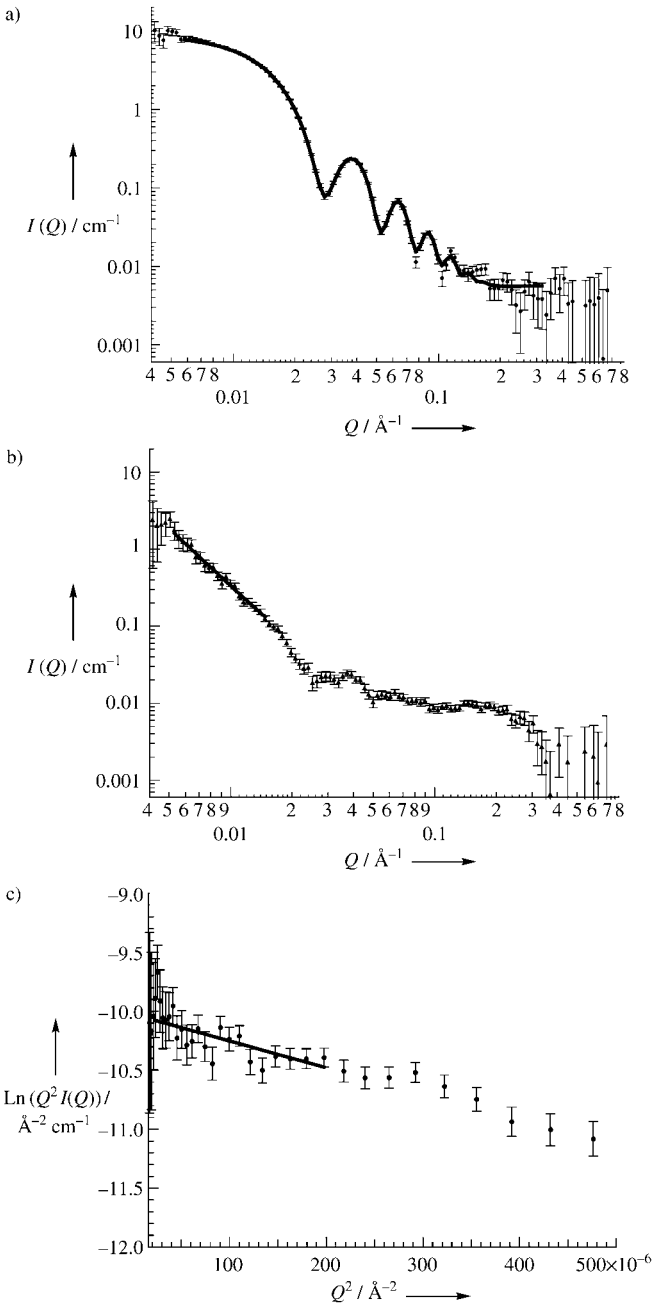

Figure 2. SANS data of a) CPMV particles in D_2O buffer along with a spherical-shell fit and b) CPMV–particle assemblies at the interfaces between the perfluorodecalin and buffer solutions (the H_2O/D_2O ratio is 0.313:0.687 (v/v)) to contrast match the perfluorodecalin. c) Modified Guinier analysis of scattering data from the CPMV–particle assemblies at the interfaces. The linear fit to the slope is shown in the Q region where $Q_{max} R_t < 0.6$ provides the thickness factor R_t from which the thickness t of the shell was derived using $t = \sqrt{12}\, R_t$.

$t = \sqrt{12}\, R_t$. The modified Guinier analysis of the SANS data for the CPMV assemblies demonstrates that the bioparticle assemblies at the interfaces between perfluorodecalin and H_2O/D_2O are sheetlike with $t = 16.5 \pm 1.8$ nm (Figure 2c). This analysis suggests that the CPMV forms a monolayer at the interfaces, thus assuming a uniform scattering length density for the sheets. It should be noted that no pronounced interparticle correlations were seen. At the loading of virus particles used, a low coverage of the CPMV particles at the oil and water interface is indicated by the small average thickness of the monolayer and the absence of a peak.

The wt-CPMV particles were cross-linked at the water–oil interface at 4 °C for 3 hours to lock the assembly into place by adding glutaraldehyde (ca. 2.5 wt %) into the water phase. Figure 3a shows a fluorescence confocal microscope image of a 3D reconstruction of perfluorodecalin droplets coated with wt-CPMV after cross-linking and removal of excess CPMV particles in the buffer phase by washing with water. It can be inferred from the image that the integrity of the assembly is preserved following cross-linking and the resulting capsules are not distorted in shape (see inset). Complete removal of the water and perfluorodecalin disrupts the cross-linked virus shell. Crumpled shells are observed on rehydration with the buffer solution (Figure 3b). It is likely that the perfluorodecalin evaporation and the resulting vapor pressure crushed the capsule; nevertheless, these images show that cross-linking occurred. Figure 3c depicts a spherical cap generated by the assembly and subsequent cross-linking of wt-CPMV particles around a perfluorodecalin droplet sitting on a glass slide. The cap folded backwards after complete evaporation of the solvents and washing with buffer and water, thus revealing distinct wrinkles on the surface. Several scanning force microscopy (SFM) images were taken at the edge of the back-folded cap to determine the thickness of the cross-linked virus–particle assembly. The inset of Figure 3c shows the site where the SFM image in Figure 3d was taken. Cross-sectional analysis, averaged over 256 scan lines, yields a step height of 29 ± 2 nm, which is consistent with a monolayer formed by virus particles 28–32 nm in diameter. The concentration of CPMV particles adsorbed at the interface is much larger than the concentration of residual particles in solution, even though the cross-linking is initiated from the buffer phase, thus leading to preferential cross-linking at the water–oil interface. The low reaction temperature and slow rate of reaction provides further control over the process. The SFM image in Figure 3d shows that closely packed individual CPMV particles can be distinguished, even after cross-linking. Thus, the glutaraldehyde reaction has been shown to induce cross-linking and produce well-defined, robust, and cross-linked virus–particles assemblies.

An even higher level of control over the cross-linking reaction can be achieved with biotin/avidin binding. A CPMV mutant with an inserted cysteine residue was employed to provide orthogonal reactive sites, which were amino groups of the native lysines and thiol groups of the inserted cysteines.[33,34] Doubly labeled virus particles were afforded by attaching biocytin maleimide (**3**) to the surface cysteine units of the virus and then carrying out fluorescent labeling at the lysine moieties (Scheme 2). Avidin has four binding sites for biotin, which allows well-controlled cross-linking of the biotin-modified CPMV particles at interfaces. Figure 4a shows a 3D reconstruction of a series of fluorescence confocal microscope images of the CPMV/biotin assembly around perfluorodecalin droplets cross-linked with avidin for 3 hours at 4 °C. Relative to the glutaraldehyde cross-linking, no desorption of the virus particles is observed after removal of

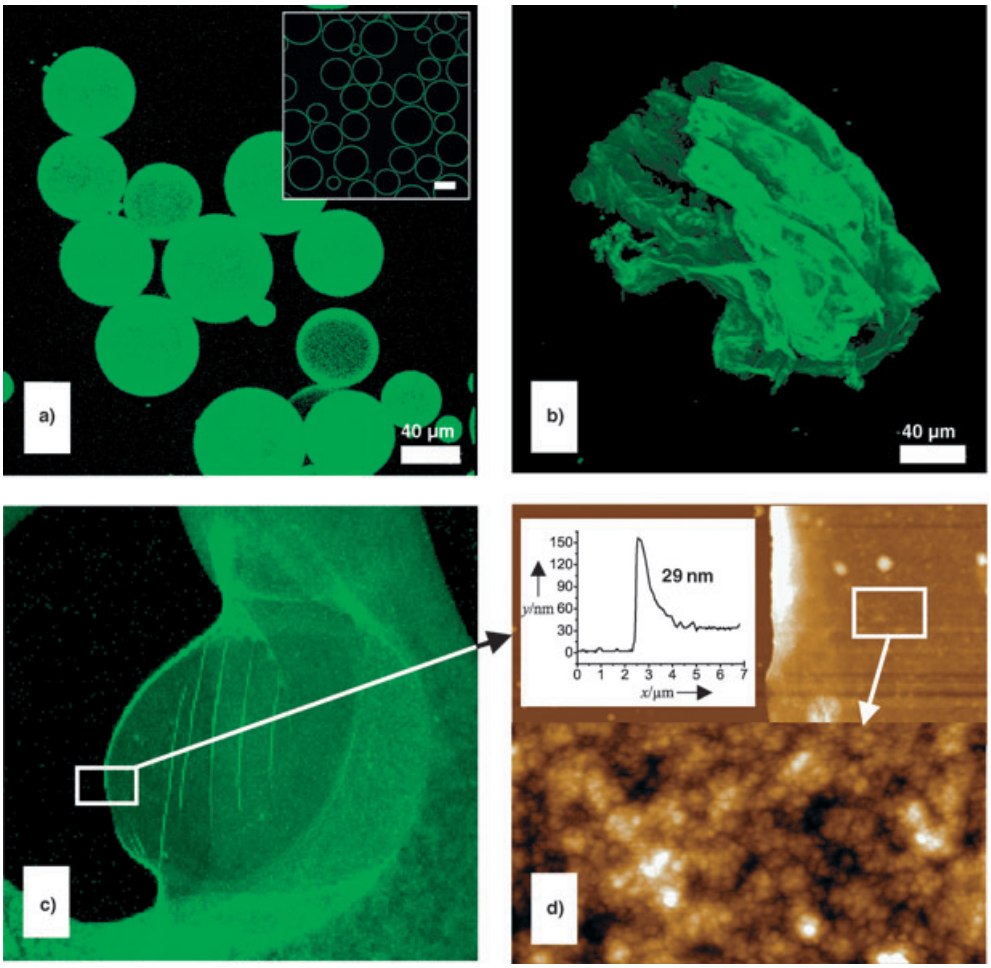

Figure 3. Confocal fluorescence microscope image of CPMV–particle assembly after cross-linking with glutaraldehyde. a) Three-dimensional reconstruction of perfluorodecalin droplets in water that are coated with the virus (inset: cross-sectional view). Excess particles were removed by successive washing with water. b) Crumpled droplet after complete drying and rehydration with water. c) Capsule cap after complete drying. d) The white box shows the area at which the SFM scan was taken, and the lower part shows the height profile on top of the collapsed capsule (image width = 2 µm, *z* range = 30 nm).

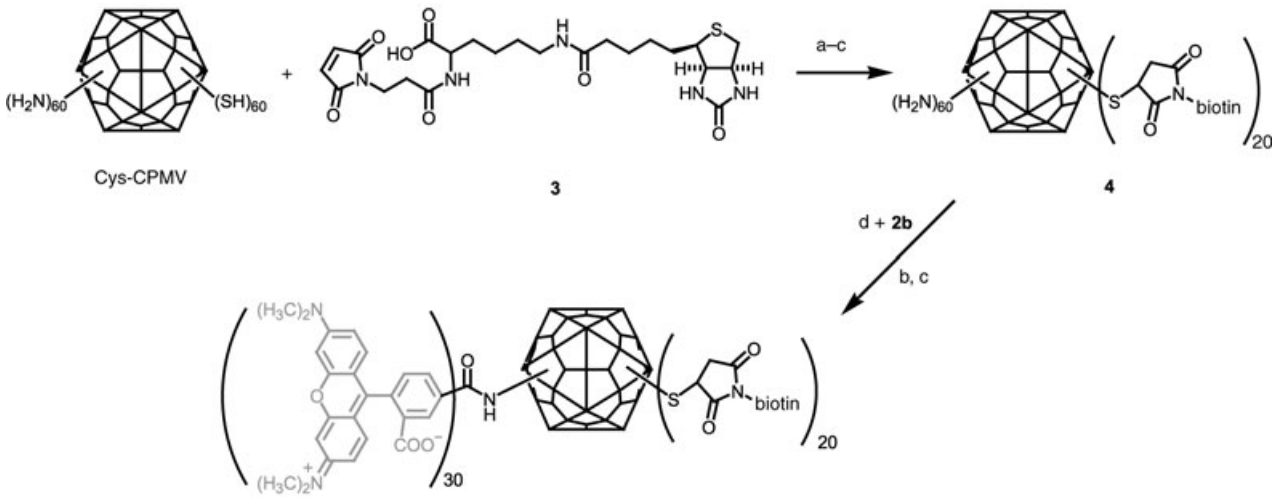

Scheme 2. The formation of doubly labeled Cys-CPMV particles. a) 20% DMSO in buffer, pH 6.0, 4 °C, 24 h; b) ultracentrifugation; c) dialysis; d) 20% DMSO in buffer, pH 7.0, 4 °C, 24 h.

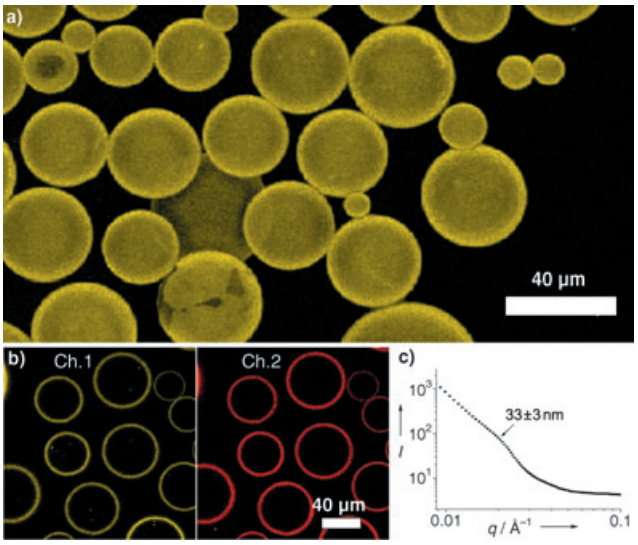

Figure 4. a) A 3D reconstruction of a confocal fluorescence microscope image of perfluorodecalin droplets that are coated with CPMV/biotin after being cross-linked with avidin for 3 h at 4 °C. Excess particles were removed by successive washing with water. b) A two-channel confocal fluorescence microscope image of particle assemblies after cross-linking with fluorescently tagged streptavidin: Channel 1 (yellow, left side) shows the CPMV/biotin fluorescence and channel 2 (red, right side) shows the ATTO-655-streptavidin fluorescence. c) SAXS data of the cross-linked CPMV/biotin shell around the perfluodecalin droplets.

the excess particles by successive washing with water; moreover, the integrity of the capsule shell is retained after the reaction. Nevertheless, evidence for cracks and holes can be found in some of the shells, but the crack characteristics of the capsules in the lower left corner are typical for a solid shell. Figure 4b shows a two-channel confocal fluorescence microscope image of particle assemblies after cross-linking with fluorescently tagged streptavidin. The labeled fluorescence from the particles is seen as yellow and the fluorescence from Atto-655-Streptavidin is seen at the interface as red. Small-angle X-ray scattering (SAXS) data of the cross-linked CPMV/biotin shell around the perfluorodecalin droplets exhibit a weak first order shoulder that corresponds to a *d*-spacing of 33 ± 3 nm (Figure 4c); however, a second order could not be resolved. This interparticle correlation distance is in agreement with the virus–particle diameter of 28–32 nm. We note that the SFM experiments, identical to those performed when the cross-linking was carried out with glutaraldehyde, yielded values for the shell thicknesses that were in agreement with the expected CPMV–monolayer dimension.

The mechanical properties of these cross-linked bionanoparticle assemblies were investigated by atomic force microscopy (AFM). An AFM molecular-force probe mounted on an inverted Olympus IX71 microscope was used, as described in detail previously.[38] For the effective application of AFM force-spectroscopic anaylsis to oil droplets in a water matrix, the droplets were allowed to settle to the bottom of the observation chamber and attach to the polyallylamine-coated glass substrate. The high density of perfluoroctane relative to water promotes rapid sedimentation, and the polyallylamine coating promotes droplet adhesion. Force-deformation measurements were performed on the droplets with particle assemblies that were both non-cross-linked and cross-linked using glutaraldehyde. A typical set of force-deformation data is shown in Figure 5a, along with the statistics of the droplet-

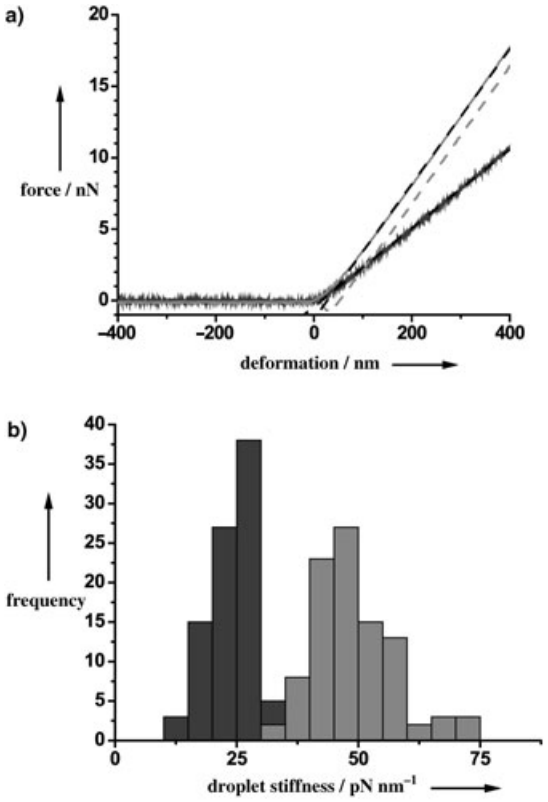

Figure 5. a) A typical force-deformation curve for a droplet of similar size without cross-linking (left) and with cross-linking (right) of virus–particle assemblies. The slope of the linear fit of the force-deformation curves in the linear regime (broken black line) corresponds to the droplet stiffness. b) Statistics of the droplet stiffness for a large number of measurements. Left: non-cross-linked; right: cross-linked.

stiffness measurements for a large number of droplets (Figure 5b). These data clearly indicate that cross-linking of the bionanoparticle assemblies on the surface of the droplets results in an increase in the droplet stiffness. The droplet stiffness is determined by measuring the slope of the force-deformation curves in the linear regime. We note that the deformation behavior of the nanoparticle assemblies is not only determined by membrane bending and stretching, but also by the surface tension of the particle-covered interface. A model that quantifies the force-deformation data in terms of effective surface tension and membrane stiffness will be published separately.

In summary, it has been shown that CPMV nanoparticles self-assemble as a monolayer at perfluorodecalin–water interfaces. These close-packed assemblies were successfully cross-linked by using two different well-defined cross-linking approaches. These reactions did not disrupt the integrity of the virus–particle assemblies, but rather strengthened the

assembly by formation of a robust membrane with covalent inter-bionanoparticle connectivity. The crumpling of the capsules points to the formation of mechanically robust membranes of CPMV particles that are cross-linked. The assembly of these particles at fluid–fluid interfaces provides opportunities for their use in different applications while further chemical functionalization can be performed.

Experimental Section

Generation of CPMV: wt-CPMV and Cys-CPMV mutants were generated as reported previously.[31–33] Virus concentrations were determined by measuring the absorbance at 260 nm (a concentration of 1.0 mg mL^{-1} gives a standard absorbance of 0.8). The average molecular weight of the wt-CPMV virion is 5.6×10^6 Da.

2a and **2b**: A solution of *N*-hydroxysuccinimide ester (**1a** or **1b**, 5 μmol) in DMSO (2 mL) was introduced into a solution of wt-CPMV (10 mg) in potassium phosphate buffer (8 mL, pH 7.0). The reaction mixture was purified after incubation at 4 °C for 24 h by ultracentrifugation at 42000 rpm over a 1.0-cm-high sucrose cushion, followed by resuspension in potassium phosphate buffer (2 mL, pH 7.0). The recovery of derivatized viruses was typically 60–80 %, and all such samples were composed of > 95 % intact particles. Dialysis over the buffer (4 L) was performed with a 10-kD cut-off membrane (Pierce) to remove any remaining organic reagent. Dye loadings were obtained by measuring the absorbance at λ_{max} and using known molar absorptivities. On average, 60 dye molecules were loaded onto one viral particle.

5: A solution of biocytin maleimide (**3**, 5 μmol) in DMSO (2 mL) was added to a solution of Cys-CPMV mutant[33] (10 mg) in potassium phosphate buffer (8 mL, pH 6.0). The reaction mixture was purified after incubation at 4 °C for 24 h by ultracentrifugation at 42000 rpm over a 1.0-cm-high sucrose cushion. The pellet was dissolved in potassium phosphate buffer (2 mL, pH 7.0) to afford **4**, which was then treated with *N*,*N*,*N*′,*N*′-tetramethylrhodamine (**2b**) in a similar fashion to wt-CPMV. The recovery of derivatized viruses was typically 45–60 %, and all such samples were composed of > 95 % intact particles. Dialysis over the buffer (4 L) was performed with a 10-kD snake-skin dialysis membrane (Pierce) to remove any remaining organic reagent. Dye loading was determined by measurement of the absorbance at λ_{max} and using known molar absorptivities. The loading of biotin was determined by a parallel reaction with 5-maleimidofluorescein. About 20 biotin and 30 dye molecules could be loaded in a typical reaction to one viral particle.

Assembly and cross-linking: The assembly experiments were conducted with fluorescently tagged wt-CPMV particles. The CPMV stock solution (ca. 5 mg mL^{-1}) was diluted 20 times with potassium phosphate buffer (0.1 M, pH 7.0) to give a 0.25 mg mL^{-1} solution. Perfluorodecalin (0.03 mL) was added to the CPMV solution (0.3 mL) and the particles were allowed to assemble for 2–3 h at 4 °C. Glutaraldehyde (15 μL, 50 % in water (v/v)) was then added to cross-link the virus–particle assembly. The addition was carried out at 4 °C and the reaction mixture incubated for 3 h. The CPMV/biotin assemblies were prepared in the same way and cross-linked with avidin (30 μL of a 2 mg mL^{-1} stock solution) with incubation at 4 °C for 3 h. Excess particles in the buffer phase were removed after cross-linking by subsequent washing with water.

Laser scanning confocal microscopy (LSCM) analysis: The LSCM images were taken on a Leica TCS SP2 LSCM with excitation by an Ar laser and HeNe laser. The fluorescence from the virus nanoparticles or the fluorescently tagged streptavidin is shown by a color scale, in which brightness represents intensity.

Tensiometer measurements: The changes in the interfacial tension between the bionanoparticle solution and the oil phase were determined at room temperature with an OCA 20 Dataphysics pendant-drop tensiometer with video camera for drop-image processing, which allows rapid drop-image acquisition, edge detection, and fitting of the Young–Laplace equation.

SFM analysis: SFM images were taken on a Digital Instruments Dimension 3100 microscope operated in the tapping mode (the free amplitude of the cantilever was approximately 20 nm and the amplitude set point was approximately 0.98). The standard silicon nitride probes were driven at 3 % offset below their resonance frequencies in the range of 250–350 kHz. Height and phase images were taken at scanning speeds of around 6 μm s^{-1}.

SANS analysis: SANS experiments were carried out by time-of-flight small-angle neutron diffractometry (SAND)[39,40] at the Intense Pulsed Neutron Source (Argonne National Laboratory, Argonne, IL) using neutrons with wavelengths of 0.9–14 Å at a sample-to-detector distance of 2.0 m. SAND provides data in the Q range of 0.0035–1.0 Å^{-1} in a single measurement, in which the Q value is related to the neutron wavelength λ and the scattering angle 2θ by $Q = 4\pi \sin\theta/\lambda$. The samples were measured in suprasil sample cells with a path length of 2 mm. The data for each sample were corrected for the instrumental background, solvent scattering (for dispersed bioparticles only and not for the bioparticle-coated microemulsions), and detector nonlinearity. The data were then placed on an absolute scale.

Synchrotron SAXS analysis: Synchrotron SAXS measurements were performed with the ID15 beamline equipment at the Advanced Photon Source (Argonne National Laboratory, Argonne, IL). The operating beam energy was 12.5 keV, which corresponds to a peak wavelength of 0.1 nm, and the beam size was 300×300 μm^2. A Bruker CCD detector, housed in a 2-m evacuated flight tube, was used to acquire 1024×1024 pixels images with typical exposure times of around 1 s.

Force spectroscopic analysis: The AFM studies were performed with a Molecular-Force Probe (Asylum Research, Santa Barbara, CA) mounted on an inverted optical microscope (Zeiss Axiomat 200, Zeiss, Oberkochen, Germany). This combination enabled us to position the AFM tip on the area of interest of our sample, which in our case was directly on the top of the emulsion droplets, as well as perform simultaneous quantitative microinterferometry (RICM) experiments.[38] We used the colloidal probe technique[41,42] instead of using a sharp tip for probing the droplets, which has the advantage of providing a defined and reproducible contact geometry and avoids membrane failure because of penetration by a sharp tip. We used some tipless cantilevers (Micromash, Estonia) with a nominal spring constant of 0.08 N m^{-1} on which glass beads of 30–50 μm (Polysciences, Warrington, PA) were fixed using epoxy glue (UHU Plus endfest 300). The cantilevers were plasma-cleaned (PDC-32G, Harrick Scientific Corporation, NY) before mounting on the AFM head for 1 min at a pressure lower than 1 mbar. The force constant for each cantilever was calibrated by using the method of Sader[43,44] and measuring the thermally induced motion of the unloaded cantilever.[45,46] Experiments (at ca. 23 °C) were typically done at imposed displacement rates of 300 nm s^{-1}.

Received: November 17, 2004
Published online: April 1, 2005

Keywords: bionanoparticles · interfaces · membranes · self-assembly · viruses

[1] X. Duan, Y. Huang, Y. Cui, J. Wang, C. M. Lieber, *Nature* **2001**, *409*, 66.
[2] Y. Huang, X. Duan, Q. Wei, C. M. Lieber, *Science* **2001**, *291*, 630.
[3] G. M. Whitesides, B. Grzybowski, *Science* **2002**, *295*, 2418.
[4] S. Paul, C. Pearson, A. Molloy, M. A. Cousins, M. Green, S. Kolliopoulou, P. Dimitrakis, P. Normand, D. Tsoukalas, M. C. Petty, *Nano Lett.* **2003**, *3*, 533.
[5] Y. Lin, H. Skaff, T. Emrick, A. D. Dinsmore, T. P. Russell, *Science* **2003**, *299*, 226.

[6] Y. Lin, H. Skaff, A. Böker, A. D. Dinsmore, T. Emrick, T. P. Russell, *J. Am. Chem. Soc.* **2003**, *125*, 12690.
[7] S. U. Pickering, *J. Chem. Soc.* **1907**, 2001.
[8] R. Aveyard, B. P. Binks, J. H. Clint, *Adv. Colloid Interface Sci.* **2003**, *100*, 503.
[9] F. H. C. Crick, J. D. Watson, *Nature* **1956**, *177*, 473.
[10] L. Liljas, *Curr. Opin. Struct. Biol.* **1999**, *9*, 129.
[11] J. E. Johnson, V. Chiu, *Curr. Opin. Struct. Biol.* **2000**, *10*, 229.
[12] K. S. Raja, Q. Wang in *Encyclopedia of Nanoscience and Nanotechnology* (Ed.: K. Puryera), Marcel Dekker, New York, **2004**, p. 321.
[13] B. K. Jap, M. Zulauf, T. Scheybani, A. Hefti, W. Baumeister, U. Aebi, A. Engel, *Ultramicroscopy* **1992**, *46*, 45.
[14] P. Fromherz, *Nature* **1971**, *231*, 267.
[15] K. Aoyama, K. Ogawa, Y. Kimura, Y. Fujiyoshi, *Ultramicroscopy* **1995**, *57*, 345.
[16] E. E. Uzgiris, R. D. Kornberg, *Nature* **1983**, *301*, 125.
[17] T. Scheybani, H. Yoshimura, W. Baumeister, K. Nagayama, *Langmuir* **1996**, *12*, 431.
[18] I. Yamashita, *Thin Solid Films* **2001**, *393*, 12.
[19] H. Yoshimura, T. Scheybani, W. Baumeister, K. Nagayama, *Langmuir* **1994**, *10*, 3290.
[20] P. Pieranski, *Phys. Rev. Lett.* **1980**, *45*, 569.
[21] O. D. Velev, K. Furusawa, K. Nagayama, *Langmuir* **1996**, *12*, 2374.
[22] X. Zhai, S. Efrima, *J. Phys. Chem.* **1996**, *100*, 11019.
[23] B. P. Binks, J. H. Clint, *Langmuir* **2002**, *18*, 1270.
[24] A. D. Dinsmore, M. F. Hsu, M. G. Nikolaides, M. Marquez, A. R. Bausch, D. A. Weitz, *Science* **2002**, *298*, 1006.
[25] D. J. Siler, J. Babcock, G. Bruening, *Virology* **1976**, *71*, 560.
[26] G. P. Lomonossoff, J. E. Johnson, *Prog. Biophys. Mol. Biol.* **1991**, *55*, 107.
[27] G. P. Lomonossoff, J. E. Johnson, *Curr. Opin. Struct. Biol.* **1996**, *6*, 176.
[28] G. P. Lomonossoff, M. Shanks, C. L. Holness, A. J. Maule, D. Evans, Z. Chen, C. Stauffacher, J. Johnson in "Comovirus Capsid Proteins: Synthesis, Structure, and Evolutionary Implications" in *Biochem. Mol. Biol. Plant-Pathog. Interact.*, *Vol. 32* (Ed.: C. J. Smith), Clarendon, Oxford, **1991**, pp. 76.
[29] T. W. Lin, Z. G. Chen, R. Usha, C. V. Stauffacher, J. B. Dai, T. Schmidt, J. E. Johnson, *Virology* **1999**, *265*, 20.
[30] Q. Wang, T. R. Chan, R. Hilgraf, V. V. Fokin, K. B. Sharpless, M. G. Finn, *J. Am. Chem. Soc.* **2003**, *125*, 3192.
[31] Q. Wang, E. Kaltgrad, T. W. Lin, J. E. Johnson, M. G. Finn, *Chem. Biol.* **2002**, *9*, 805.
[32] Q. Wang, T. Lin, L. Tang, J. E. Johnson, M. G. Finn, *Angew. Chem.* **2002**, *114*, 477; *Angew. Chem. Int. Ed.* **2002**, *41*, 459.
[33] Q. Wang, T. W. Lin, J. E. Johnson, M. G. Finn, *Chem. Biol.* **2002**, *9*, 813.
[34] Q. Wang, K. S. Raja, K. D. Janda, T. Lin, M. G. Finn, *Bioconjugate Chem.* **2003**, *14*, 38.
[35] S. Meunier, E. Strable, M. G. Finn, *Chem. Biol.* **2004**, *11*, 319.
[36] G. Porod, *Small Angle X-Ray Scattering*, Academic Press, London, **1982**, pp. 17.
[37] J. M. Gallas, K. C. Littrell, S. Seifert, G. W. Zajac, P. Thiyagarajan, *Biophys. J.* **1999**, *77*, 1135.
[38] F. Dubreuil, N. Elsner, A. Fery, *Europhys. J. E* **2003**, *12*, 215.
[39] P. Thiyagarajan, V. Urban, K. Littrell, C. Ku, D. G. Wozniak, H. Belch, R. Vitt, J. Toeller, D. Leach, J. R. Haumann, G. E. Ostrowski, L. I. Donley J. Hammonds, J. M. Carpenter, R. K. Crawford, in *ICANS-XIV, 14th Meeting of the International Collaboration on Advanced Neutron Sources*, *Vol. XIV*, Starved Rock Lodge, Utica, IL, **1998**, Vol. 2, p. 864.
[40] P. Thiyagarajan, J. E. Epperson, R. K. Crawford, J. M. Carpenter, T. E. Klippert, D. G. Wozniak, *J. Appl. Crystallogr.* **1997**, *30*, 280.
[41] W. A. Ducker, T. J. Senden, R. M. Pashley, *Nature* **1991**, *353*, 239.
[42] H. J. Butt, *Biophys. J.* **1991**, *60*, 1438.
[43] J. E. Sader, *J. Appl. Phys.* **1998**, *84*, 64.
[44] J. E. Sader, J. W. M. Chon, P. Mulvaney, *Rev. Sci. Instrum.* **1999**, *70*, 3967.
[45] H. J. Butt, M. Jaschke, *Nanotechnology* **1995**, *6*, 1.
[46] J. L. Hutter, J. Bechhoefer, *Rev. Sci. Instrum.* **1993**, *64*, 1868.

